Supplementary Information (SI) for Materials Advances.
This journal is © The Royal Society of Chemistry 2026

SUPPORTING INFORMANTION

Harnessing the Untapped Potential of Lanthanide-based Perovskite ($RbYbCl_3$) Absorber: From Material Properties to Device Implementation

Md. Sajjadur Rahman[a], Akram Hossan Mahedi[a], Mohammad Yasin Hayat Khan[a], Md. Tarekuzzaman[a], Md. Hasan Mia [a,b], Sohail Ahmad[c], Md. Rasheduzzaman[a], Md. Zahid Hasan[a*]

[a] Materials Research and Simulation Lab, Department of Electrical and Electronic Engineering, International Islamic University Chittagong, Kumira, Chittagong, 4318, Bangladesh
[b] Department of Computer and Communication Engineering, International Islamic University Chittagong, Kumira, Chittagong, 4318, Bangladesh
[c] Department of Physics, College of Science, P O Box 9004, King Khalid University, Abha, Saudi Arabia

[*]**Corresponding Author; zahidhasan.02@gmail.com (Md. Zahid Hasan)**

Table S1: Electron transport layer's (ETLs) parameters

Table S2: Hole transport layer's (HTLs) parameters

Fig. S2: Variation of photovoltaic performance parameters as a function of the absorber bandgap for perovskite solar cells employing (a) IGZO, (b) SnS_2, (c) WO_3, and (d) ZnO as the electron transport layer.

Fig. S3: Dependence of key photovoltaic performance parameters on the absorber electron affinity for perovskite solar cells with (a) IGZO, (b) SnS_2, (c) WO_3, and (d) ZnO electron transport layers.

Fig. S4: Effect of absorber electron mobility variation on photovoltaic performance parameters ($V_{OC,}$ J_{SC}, FF and PCE) for perovskite solar cells using (a) IGZO, (b) SnS_2, (c) WO_3, and (d) ZnO as the electron transport layer.

Fig. S5: Influence of absorber hole mobility on photovoltaic performance parameters ($V_{OC,}$ J_{SC}, FF and PCE) in perovskite solar cells incorporating (a) IGZO, (b) SnS_2, (c) WO_3, and (d) ZnO electron transport layers.

Table S1: Electron transport layer's (ETLs) parameters [1-4]

Parameters	ETLs			
	TiO_2 [1,2]	PCBM [2]	CdS [3]	ZnS [4]
Thickness (μm)	0.05	0.05	0.08	0.075
Bandgap (eV)	3.2	2	2.43	2.8
Electron Affinity (eV)	4	3.9	4.4	3.8
Permittivity (rel.)	9	3.9	10	9
Electron thermal velocity (cm/s)	1×10^{7}	1×10^{7}	1×10^{7}	1×10^{7}
Hole thermal velocity (cm/s)	1×10^{7}	1×10^{7}	1×10^{7}	1×10^{7}
CB Effective Density of States ($1/cm^3$)	2×10^{18}	2×10^{21}	2×10^{18}	2.20×10^{18}
VB Effective Density of States ($1/cm^3$)	1×10^{19}	2×10^{21}	1×10^{19}	1.80×10^{19}
Electron Mobility (cm^2/Vs)	2×10^{1}	2×10^{-01}	1×10^{2}	1×10^{2}
Hole Mobility (cm^2/Vs)	1×10^{1}	2×10^{-01}	2×10^{1}	2.5×10^{1}
Shallow Uniform Donor density ND ($1/cm^3$)	9×10^{16}	2×10^{17}	1×10^{18}	1×10^{19}
Shallow Uniform Acceptor Density NA ($1/cm^3$)	0	0	0	1×10^{6}
Total Defect Density Nt ($1/cm^3$)	1×10^{15}	1×10^{15}	1×10^{15}	1×10^{15}

Table S2: Hole transport layer's (HTLs) parameters [2,3,5-6]

Parameters	HTLs						
	CBTS [2]	**Spiro** [5]	**PTAA** [3]	**MoS_2** [3]	**CdTe** [6]	**CuI** [5]	**CuO** [5]
Thickness (μm)	0.1	0.2	0.05	0.35	0.2	0.1	0.05
Bandgap (eV)	1.9	3	2.96	1.29	1.5	3.1	1.51
Electron Affinity (eV)	3.6	2.2	2.3	4.2	3.9	2.1	4.07
Permittivity (rel.)	5.4	3	9	3	9.4	6.5	18.1
Electron thermal velocity (cm/s)	1×10^{7}	1×10^{7}	1×10^{7}	1×10^{7}	1×10^{7}	1×10^{7}	1×10^{7}
Hole thermal velocity (cm/s)	1×10^{7}	1×10^{7}	1×10^{7}	1×10^{7}	1×10^{7}	1×10^{7}	1×10^{7}
CB Effective Density of States ($1/cm^3$)	2.2×10^{18}	2.2×10^{18}	1×10^{21}	2.2×10^{18}	8×10^{17}	2.2×10^{19}	2.2×10^{19}
VB Effective Density of States ($1/cm^3$)	1.8×10^{19}	1.8×10^{19}	1×10^{21}	1.8×10^{19}	1.8×10^{19}	1×10^{19}	5.5×10^{20}
Electron Mobility (cm^2/Vs)	3×10^{1}	3.1×10^{-3}	1×10^{1}	1×10^{2}	3.2×10^{2}	1×10^{2}	1×10^{2}
Hole Mobility (cm^2/Vs)	1×10^{1}	2.1×10^{-3}	4×10^{1}	1.5×10^{2}	4×10^{1}	4.3×10^{1}	1×10^{-1}
Shallow Uniform Donor density ND ($1/cm^3$)	0	0	0	0	0	0	0
Shallow Uniform Acceptor Density NA ($1/cm^3$)	1×10^{18}	1×10^{18}	1×10^{18}	1×10^{18}	2×10^{14}	1×10^{18}	1×10^{18}
Total Defect Density Nt ($1/cm^3$)	1×10^{15}	1×10^{15}	1×10^{15}	1×10^{15}	1×10^{15}	1×10^{15}	1×10^{15}

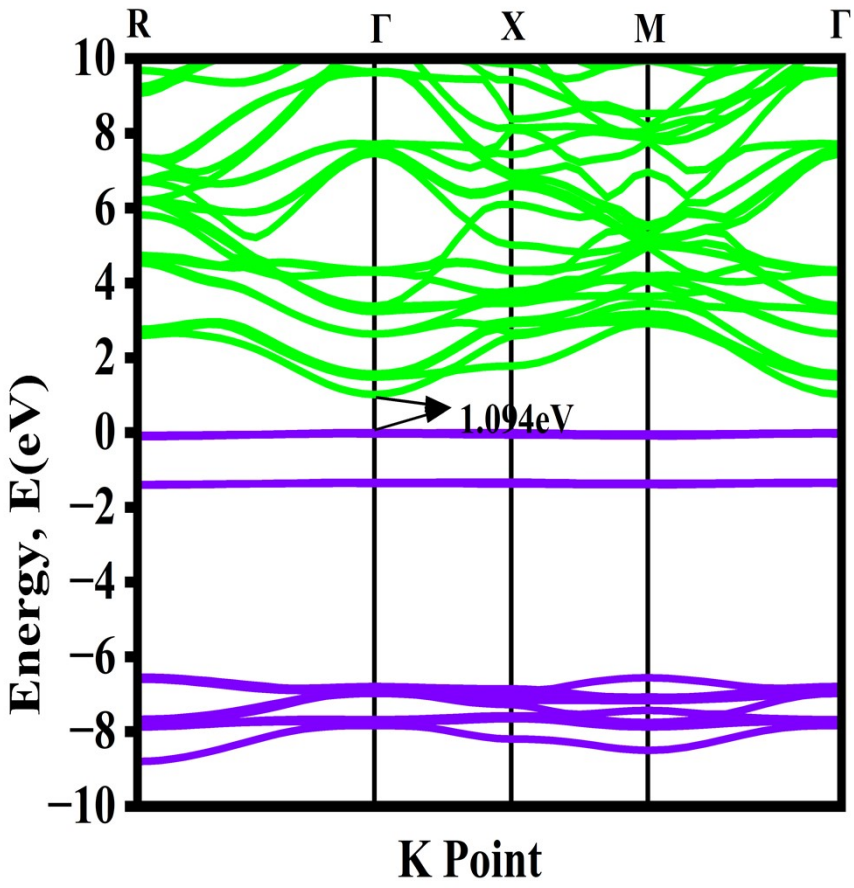

Fig. S1: Electronic band structure of $RbYbCl_3$ (PBEsol + TBmbj with SOC).

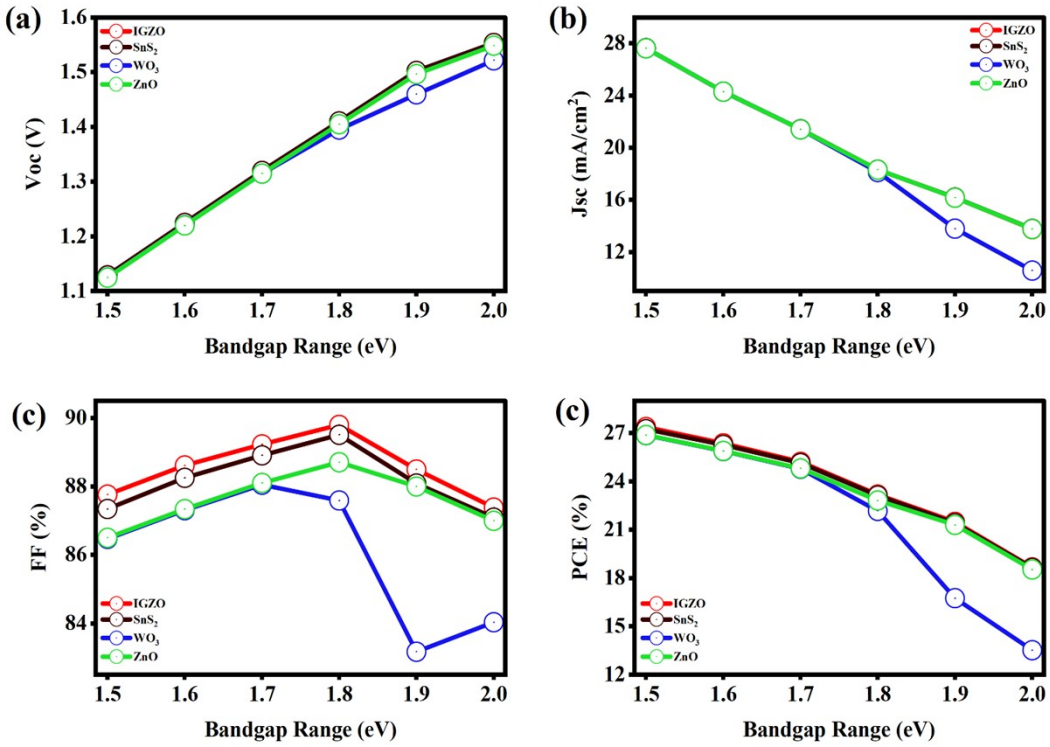

Fig. S2: Variation of photovoltaic performance parameters as a function of the absorber bandgap for perovskite solar cells employing (a) IGZO, (b) SnS_2, (c) WO_3, and (d) ZnO as the electron transport layer.

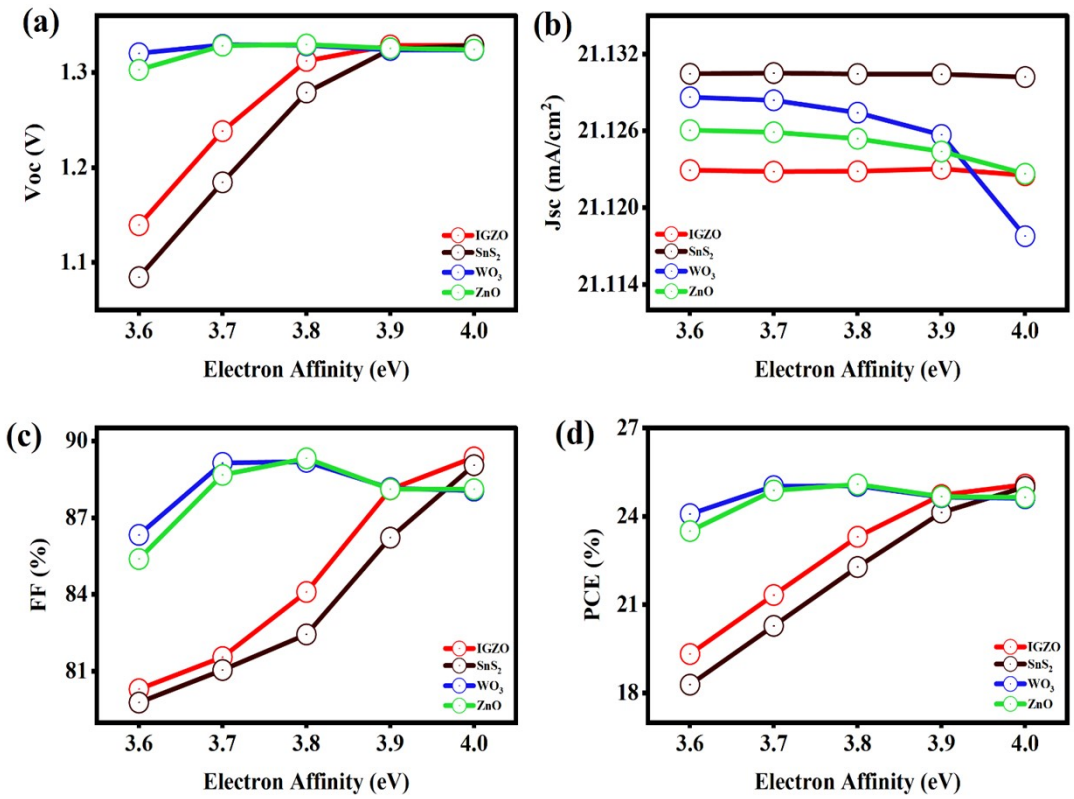

Fig. S3: Dependence of key photovoltaic performance parameters on the absorber electron affinity for perovskite solar cells with (a) IGZO, (b) SnS_2, (c) WO_3, and (d) ZnO electron transport layers.

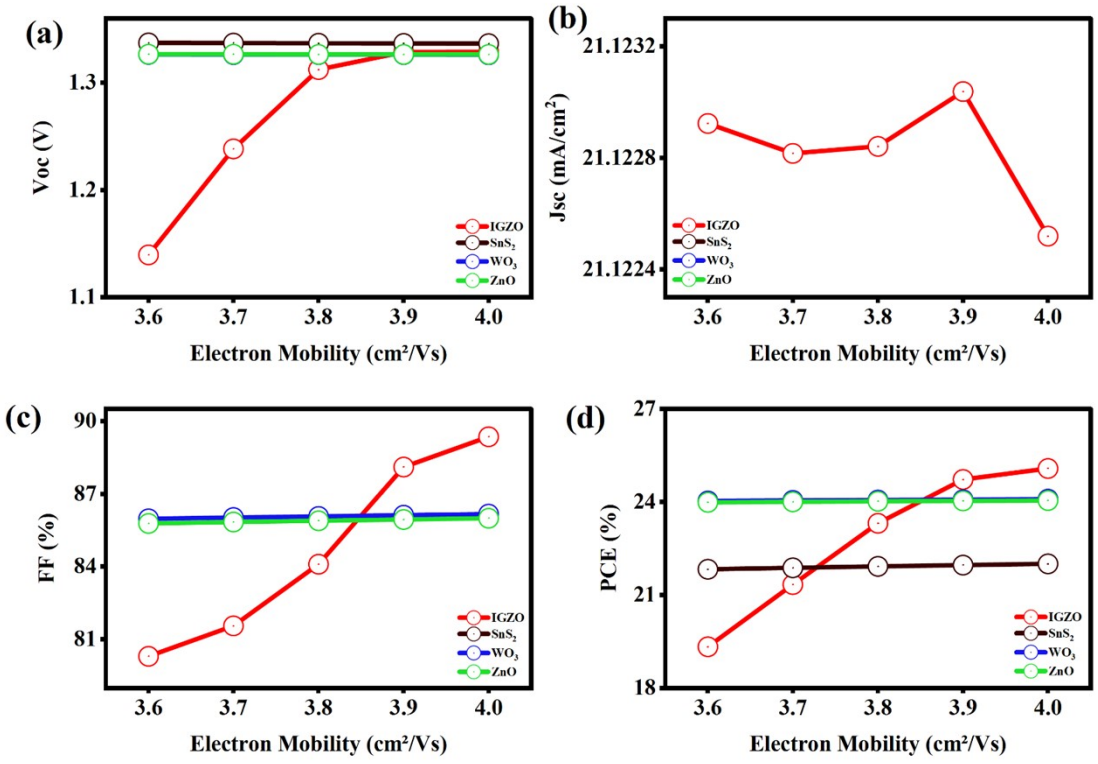

Fig. S4: Effect of absorber electron mobility variation on photovoltaic performance parameters ($V_{OC,}$ J_{SC}, FF and PCE) for perovskite solar cells using (a) IGZO, (b) SnS_2, (c) WO_3, and (d) ZnO as the electron transport layer.

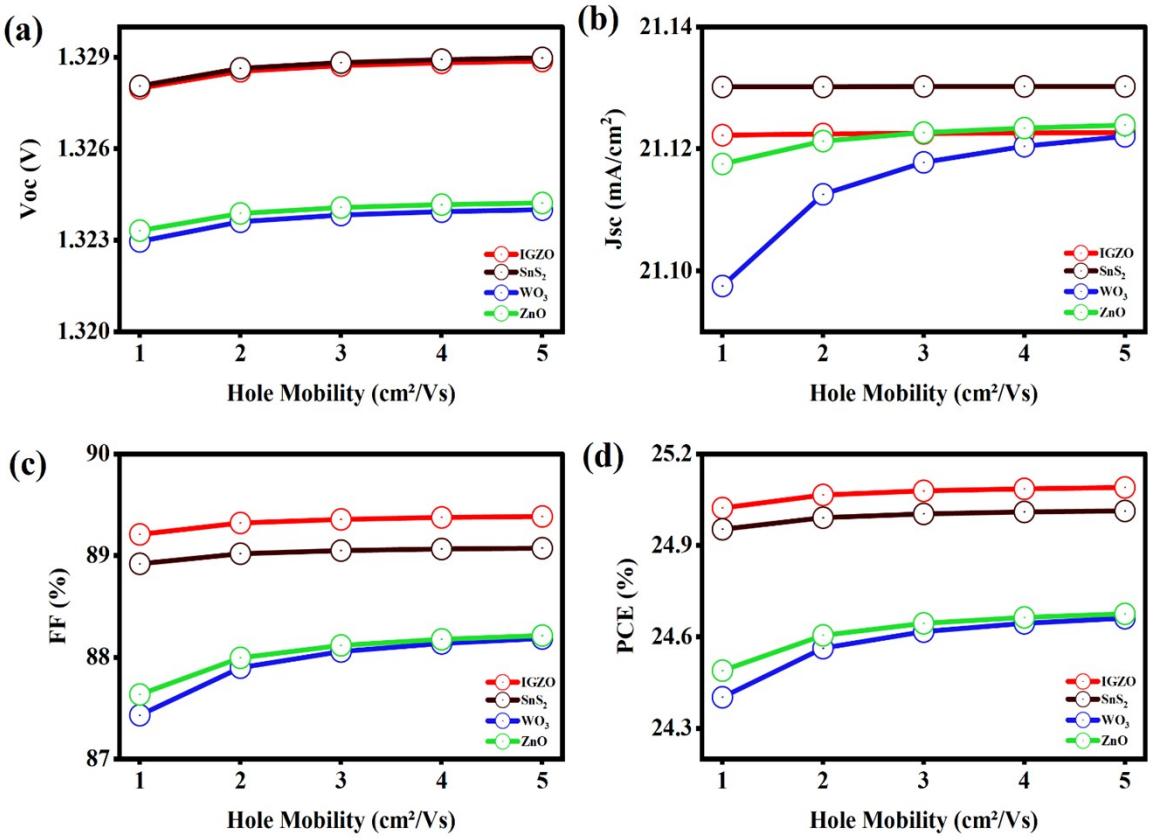

Fig. S5: Influence of absorber hole mobility on photovoltaic performance parameters ($V_{OC,}$ J_{SC}, FF and PCE) in perovskite solar cells incorporating (a) IGZO, (b) SnS_2, (c) WO_3, and (d) ZnO electron transport layers.

References:

1. M. K. Hossain, G. F. I. Toki, A. Kuddus, M. H. K. Rubel, M. M. Hossain, H. Bencherif, Md. F. Rahman, Md. R. Islam and M. Mushtaq, *Sci. Rep.*, 2023, **13**, 2521.
2. A. Hossan Mahedi, S. Uddin, M. Y. H. Khan, M. Tarekuzzaman, O. Alsalmi, M. Rasheduzzaman, S. M. G. Mostafa, M. Moazzam Hossen and M. Zahid Hasan, *RSC Adv.*, 2025, **15**, 29836–29863.
3. M. K. Hossain, M. A. Islam, M. S. Uddin, P. Paramasivam, J. A. Hamid, R. A. Alshgari, V. K. Mishra and R. Haldhar, *Sci. Rep.*, 2024, **14**, 30142.
4. M. Y. H. Khan, S. S. Hasan, Md. Z. Rahman, Md. Rasheduzzaman and Md. Z. Hasan, *RSC Adv.*, 2025, **15**, 34643–34668.
5. M. K. Hossain, M. H. K. Rubel, G. F. I. Toki, I. Alam, Md. F. Rahman and H. Bencherif, *ACS Omega*, 2022, **7**, 43210–43230.
6. M. Tarekuzzaman, M. H. Ishraq, M. S. Parves, M. A. Rayhan, S. Ahmad, M. Rasheduzzaman, K. A. A. Mamun, M. M. Hossen and M. Z. Hasan, *Phys. Chem. Chem. Phys.*, 2024, **26**, 27704–27734.